7-18-2016

Bacterial Spheroplasts as a Model for Visualizing Membrane Translocation of Antimicrobial Peptides

Lei Wei

Maria A. LaBouyer
mlabouye@wellesley.edu

Louise E. O. Darling
ldarling@wellesley.edu

Donald E. Elmore
delmore@wellesley.edu

Version: Post-print

Recommended Citation
Wei L, LaBouyer MA, Darling LEO, Elmore DE. 2016. Bacterial spheroplasts as a model for visualizing membrane translocation of antimicrobial peptides. Antimicrob Agents Chemother 60:6350–6352. doi:10.1128/AAC.01008-16.

Bacterial Spheroplasts as a Model for Visualizing Membrane Translocation of Antimicrobial Peptides

Running title: Using Spheroplasts to Visualize Peptide Translocation

Lei Wei[1], Maria LaBouyer[2], Louise E.O. Darling[1,2]*, Donald E. Elmore[1,3]*

Wellesley College

[1]Biochemistry Program, [2]Department of Biological Sciences and [3]Department of Chemistry; 106 Central St.; Wellesley, MA 02481

* To whom correspondence should be addressed:

Louise Darling

Phone: 781-283-3387

Fax: 781-283-3642

Email: ldarling@wellesley.edu

Donald Elmore

Phone: 781-283-3171

Fax: 781-283-3642

Email: delmore@wellesley.edu

Published in *Antimicrobial Agents and Chemotherapy*, **2016**, *60*:6350-6352.

Abstract:

Studies attempting to characterize the membrane translocation of antimicrobial and cell-penetrating peptides frequently are limited by the resolution of conventional light microscopy. This study shows that spheroplasts provide a valuable approach to overcome these limits. Spheroplasts produce less ambiguous images and allow for more systematic analyses of localization. Data collected with spheroplasts are consistent with studies using normal bacterial cells and imply that a particular peptide may not always follow the same mechanism of action.

Antimicrobial peptides (AMPs) represent a promising alternative to conventional therapeutics in the face of concerns about the rise of antibiotic resistant bacteria in clinical settings (1). Traditionally, AMPs were believed to kill bacteria through membrane disruption. While many AMPs do induce membrane permeabilization, researchers have identified increasing numbers of peptides that function by translocating into bacterial cells and targeting intracellular components (2). Thus, it has become increasingly important for researchers to reliably determine whether AMPs are able to effectively translocate into bacterial cells (3). Many researchers have turned to confocal microscopy in order to assess cell entry (4-11). However, bacterial cells are so small that effective imaging is limited by the resolution of conventional light microscopes. For example, in order to distinguish whether any observed signal from peptides arises from inside the cell versus on the cell membrane, researchers ideally should examine individual focal plane images throughout cells. However, if signal on the membrane is sufficiently strong it can "contaminate" slices ostensibly taken "inside" the cell, as we have observed in measurements of the membrane localized dye di-8-ANEPPS (Fig. 1).

In order to overcome these resolution limits, we have employed bacterial spheroplasts (12-14). Spheroplasts are produced by culturing bacteria in the presence of an antibiotic, such as cephalexin, that prevents division while still allowing cells to grow. The resulting elongated bacterial "snakes" are then exposed to lysozyme, which digests the outer cell wall and produces spherical spheroplasts that are typically 2-5 μm in diameter (Supplemental Figure 1). Perhaps even more important than larger size, the spherical shape allows one to obtain consistent slices regardless of how a spheroplast is oriented during imaging.

In order to test the validity of using spheroplasts to assess peptide translocation, we have measured the cellular localization of four previously characterized peptides (Table 1). To this end, we exposed *E. coli* spheroplasts to peptides with an N-terminally conjugated FITC label for imaging; detailed methods for spheroplast preparation and peptide incubation are provided as Supplemental Information. As one set of positive and negative controls, we chose buforin II (BF2), arguably the best studied membrane translocating AMP (15), and BF2 with a P11A mutation that dramatically decreases the peptide's ability to enter cells and lipid vesicles (6, 16). As an additional non-translocating control we employed magainin 2, a prototypical AMP that acts at the cell membrane (16). As in previous studies, BF2 and magainin peptides included F10W or F5W variations, respectively, which allow for straightforward quantification without significantly altering peptide activity or mechanism. We also considered HipC, a cell-penetrating peptide without antibacterial activity that was previously observed to enter *E. coli* (5).

All four control peptides showed the same behavior in spheroplasts as when studied with normal *E. coli* cells (Fig. 2). Both BF2 and HipC clearly showed entry into the majority of spheroplasts, while P11A BF2 and magainin typically co-localized with membrane dye. For all samples, we found that the use of a membrane dye made it significantly easier to visually distinguish membrane localization from cytosol entry, and no samples showed membrane dye signal contamination on image slices taken from the inside of spheroplasts, regardless of dye intensity.

In addition to providing improved confocal images, working with spheroplasts also allows us to obtain appreciably more individual images than possible when working with normal cells. While the smaller samples of images possible with bacterial cells can allow one to demonstrate

qualitative trends, the difficulty of obtaining sufficiently high-quality images makes it infeasible to perform more systematic analyses of entry data. However, with spheroplasts we can consider the percentage of images showing translocation or membrane localization, providing more systematic data (Table 1). Again, these percentages support the previously observed trends for membrane entry (5, 6, 16), with BF2 and HipC entering significantly more spheroplasts than P11A BF2 and magainin. Interestingly, none of these peptides exclusively exhibit membrane localization or membrane translocation behavior. It is possible that spheroplast behavior differs from bacterial cells or that the observed heterogeneity was related to the exact time of imaging—for example, perhaps all spheroplasts would show entry with BF2 if allowed to incubate for a longer time. However, our observation could also be consistent with the idea that a given AMP may not always follow a single, exclusive mechanism. In fact, there is some evidence for this in previous studies, such as measurements that show the "translocating" BF2 peptide does induce low levels of membrane permeabilization (17), and that the P11A mutation in BF2 reduces but does not eliminate translocation into lipid vesicles (16). It will be interesting for future studies on spheroplasts, bacterial cells, and other model systems to further evaluate this possibility. It is also worth noting that it is impossible to know for certain whether a particular spheroplast is alive, in the process of dying or dead in our images based on the timeframe between peptide incubation and mounting and focusing a slide. While this limitation also occurs for studies with normal bacteria, the optical advantages of spheroplasts may make studies looking at the timeframe of AMP effect on cells more feasible.

In summary, bacterial spheroplasts provide a promising approach for the effective visualization of AMP interactions with bacterial cells. Clearly, there are differences between "normal"

bacterial cells and spheroplasts, in particular the lack of the outer cell wall. Researchers will need to take care to ensure that the lack of cell wall does not affect the results observed in spheroplast experiments for peptides. For example, the cell wall may have a "sieving" effect with some larger peptides that would be lost in spheroplasts, requiring additional controls comparing spheroplasts and "normal" cells in other assays (18). However, even with these caveats we believe spheroplasts provide an excellent model system compared to other alternatives to overcome size and shape limitations, such as giant unilamellar vesicles (19-21), as spheroplasts preserve a physiological bacterial membrane composition and are viable if returned to growth conditions (13, 22). Moreover, although spheroplasts have generally been produced from *E. coli,* protocols can be adjusted to make them from other strains (23). Thus, we believe the use of bacterial spheroplasts can be a useful addition to the toolbox of researchers characterizing AMPs and other membrane active agents, such as cell-penetrating peptides.

References

1. **Wang, G., B. Mishra, K. Lau, T. Lushnikova, R. Golla, and X. Wang**, 2015 Antimicrobial peptides in 2014. Pharmaceuticals **8**:123-150.
2. **Hale, J.D. and R.E. Hancock**, 2007 Alternative mechanisms of action of cationic antimicrobial peptides on bacteria. Expert Review of Anti-Infective Therapy **5**:951-959.
3. **Henriques, S.T., M.N. Melo, and M.A. Castanho**, 2007 How to address CPP and AMP translocation? Methods to detect and quantify peptide internalization in vitro and in vivo (Review). Mol Membr Biol **24**:173-84.
4. **Libardo, M.D., J.L. Cervantes, J.C. Salazar, and A.M. Angeles-Boza**, 2014 Improved bioactivity of antimicrobial peptides by addition of amino-terminal copper and nickel (ATCUN) binding motifs. ChemMedChem **9**:1892-901.
5. **Bustillo, M.E., A.L. Fischer, M.A. LaBouyer, J.A. Klaips, A.C. Webb, and D.E. Elmore**, 2014 Modular analysis of hipposin, a histone-derived antimicrobial peptide consisting of membrane translocating and membrane permeabilizing fragments. BBA–Biomembranes **1838**:2228-33.
6. **Park, C.B., K.S. Yi, K. Matsuzaki, M.S. Kim, and S.C. Kim**, 2000 Structure-activity analysis of buforin II, a histone H2A-derived antimicrobial peptide: The proline hinge is responsible for the cell-penetrating ability of buforin II. Proceedings of the National Academy of Sciences of the United States of America **97**:8245-8250.
7. **Anunthawan, T., C. de la Fuente-Nunez, R.E. Hancock, and S. Klaynongsruang**, 2015 Cationic amphipathic peptides KT2 and RT2 are taken up into bacterial cells and kill planktonic and biofilm bacteria. Biochim Biophys Acta **1848**:1352-8.

8. **Hayden, R.M., G.K. Goldberg, B.M. Ferguson, M.W. Schoeneck, M.D. Libardo, S.E. Mayeux, A. Shrestha, K.A. Bogardus, J. Hammer, S. Pryshchep, H.K. Lehman, M.L. McCormick, J. Blazyk, A.M. Angeles-Boza, R. Fu, and M.L. Cotten**, 2015 Complementary Effects of Host Defense Peptides Piscidin 1 and Piscidin 3 on DNA and Lipid Membranes: Biophysical Insights into Contrasting Biological Activities. J Phys Chem B **119**:15235-46.

9. **Shin, A., E. Lee, D. Jeon, Y.G. Park, J.K. Bang, Y.S. Park, S.Y. Shin, and Y. Kim**, 2015 Peptoid-Substituted Hybrid Antimicrobial Peptide Derived from Papiliocin and Magainin 2 with Enhanced Bacterial Selectivity and Anti-inflammatory Activity. Biochemistry **54**:3921-31.

10. **Koo, Y.S., J.M. Kim, I.Y. Park, B.J. Yu, S.A. Jang, K.S. Kim, C.B. Park, J.H. Cho, and S.C. Kim**, 2008 Structure-activity relations of parasin I, a histone H2A-derived antimicrobial peptide. Peptides **29**:1102-1108.

11. **Pavia, K.E., S.A. Spinella, and D.E. Elmore**, 2012 Novel histone-derived antimicrobial peptides use different antimicrobial mechanisms. Biochimica Et Biophysica Acta-Biomembranes **1818**:869-876.

12. **Martinac, B., P.R. Rohde, C.G. Cranfield, and T. Nomura**, 2013 Patch clamp electrophysiology for the study of bacterial ion channels in giant spheroplasts of E. coli. Methods Mol Biol **966**:367-80.

13. **Sun, Y., T.L. Sun, and H.W. Huang**, 2014 Physical properties of Escherichia coli spheroplast membranes. Biophys J **107**:2082-90.

14. **Martinac, B., M. Buechner, A.H. Delcour, J. Adler, and C. Kung**, 1987 Pressure-sensitive ion channel in Escherichia coli. Proc Natl Acad Sci U S A **84**:2297-301.

15. **Cho, J.H., B.H. Sung, and S.C. Kim**, 2009 Buforins: Histone H2A-derived antimicrobial peptides from toad stomach. Biochim Biophys Acta **1788**:1564-1569.

16. **Kobayashi, S., K. Takeshima, C.B. Park, S.C. Kim, and K. Matsuzaki**, 2000 Interactions of the novel antimicrobial peptide buforin 2 with lipid bilayers: proline as a translocation promoting factor. Biochemistry **39**:8648-54.

17. **Cutrona, K.J., B.A. Kaufman, D.M. Figueroa, and D.E. Elmore**, 2015 Role of arginine and lysine in the antimicrobial mechanism of histone-derived antimicrobial peptides. FEBS Lett **589**:3915-20.

18. **Decad, G.M. and H. Nikaido**, 1976 Outer membrane of gram-negative bacteria. XII. Molecular-sieving function of cell wall. J Bacteriol **128**:325-36.

19. **Islam, M.Z., H. Ariyama, J.M. Alam, and M. Yamazaki**, 2014 Entry of cell-penetrating peptide transportan 10 into a single vesicle by translocating across lipid membrane and its induced pores. Biochemistry **53**:386-96.

20. **Ambroggio, E.E., F. Separovic, J.H. Bowie, G.D. Fidelio, and L.A. Bagatolli**, 2005 Direct visualization of membrane leakage induced by the antibiotic peptides: maculatin, citropin, and aurein. Biophys J **89**:1874-81.

21. **Wheaten, S.A., F.D. Ablan, B.L. Spaller, J.M. Trieu, and P.F. Almeida**, 2013 Translocation of cationic amphipathic peptides across the membranes of pure phospholipid giant vesicles. J Am Chem Soc **135**:16517-25.

22. **Ruthe, H.-J. and J. Adler**, 1985 Fusion of bacterial spheroplasts by electric fields. BBA—Biomembranes **819**:105-113.

23. **Rowe, I., M. Elahi, A. Huq, and S. Sukharev**, 2013 The mechanoelectrical response of the cytoplasmic membrane of Vibrio cholerae. J Gen Physiol **142**:75-85.

Tables

Table 1: Sequences of peptides used in the study and percentages of imaged spheroplasts showing translocation and membrane localization for each peptide. Data for each peptide was collected from a minimum of at least two independently prepared batches of spheroplasts characterized over a total of at least five separate imaging sessions for each peptide; data for each spheroplast batch is given in Supplemental Tables 1-4.

Peptide	Sequences	n of spheroplasts	% translocating	% membrane localized
BF2	TRSSRAGLQWPVGRVHRLLRK	67	63	37
P11A BF2	TRSSRAGLQWAVGRVHRLLRK	101	26	74
magainin 2	GIGKWLHSAKKFGKAFVGEIMNS	60	18	82
HipC	GNYAHRVGAGAPVWL	67	97	3

Figures

Figure 1: Confocal images from a z-stack taken of an *E. coli* cell incubated with the fluorescent membrane labeling dye di-8-ANEPPS. Z-positions are given relative to the middle image.

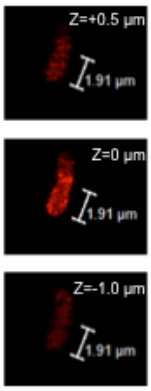

Figure 2: Confocal images of representative *E. coli* spheroplasts incubated with FITC labeled peptides (BF2, P11A BF2, HipC or magainin 2) and di-8-ANEPPS. Images from the middle of a z-stack of each spheroplast were chosen, and the merged fluorescence of FITC (green) and di-8-ANEPPS (red) is shown.

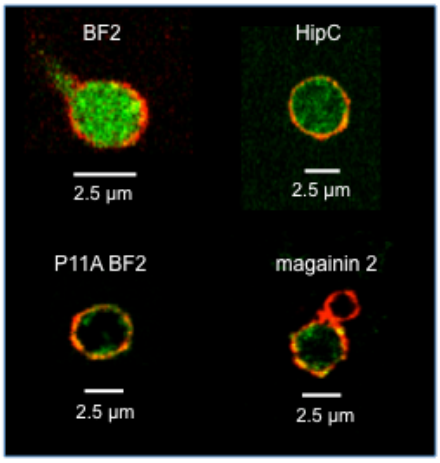

Supplemental Information for Wei et al.

Materials and Methods

Preparation of E. coli Spheroplasts

Spheroplasts were prepared from *E. coli* strain Top 10 (containing a pET45b plasmid for ampicillin resistance) in steps similar to that described in Martinac et al. (1). An overnight culture grown (37˚C in shaking incubator, approximately 148 rpm) from one plate-picked colony was diluted 1:100 in TSB liquid media in the presence of ampicillin (25 μg/mL) and allowed to grow to OD_{600} of 0.5-0.7. 3 mL of this culture was diluted 1:10 into ampicillin-containing TSB media and cephalexin was added to reach a final concentration of 60 μg/ml. The culture was then shaken at 37˚C for 2-3 hours until single-cell filaments reached sufficient length observable under light microscope at 1000x oil immersion magnification; Martinac et al. noted that filaments from 50-150 μm should produce spheroplasts 5-10 μm in diameter (1).

Filaments were harvested by centrifugation at 1500 x g for 4 minutes, and the pellet was rinsed without resuspension by gentle addition of 1 mL of 0.8 M sucrose with 1 min incubation at room temperature and then re-suspended in 3 mL of 0.8M sucrose after supernatant has been removed via pipetting. The following reagents were added in order: 150 μL of 1 M Tris Cl (pH 7.8); 120 μL of lysozyme (5mg/ml); 30 μL of Dnase I (5mg/ml); and 120 μL of 0.125 M sodium EDTA (pH 8.0). This mixture was incubated at room temperature for 6 - 10 minutes to hydrolyze the peptidoglycan layer, and spheroplast formation was followed under microscope at 1000x. 1 mL of Solution A (20 mM $MgCl_2$, 0.7 M sucrose, 10 mM Tris Cl at pH 7.8) was gradually added over a 1 minute period while stirring, and the mixture was incubated for 4 minutes at room

temperature. The mixture was layered over two separate 7-mL aliquots of Solution B (10 mM $MgCl_2$, 0.8 M sucrose, 10 mM Tris Cl at pH 7.8) previously kept on ice. These mixtures were centrifuged for 2 minutes at 1000 x g to collect spheroplasts into a pellet, and the majority of the supernatant was removed via pipetting. Spheroplast pellets were re-suspended in about 300 μL of remaining liquid.

Confocal Microscopy Imaging of Spheroplasts

Spheroplasts were either prepared immediately before or thawed from frozen stock at -80˚C and diluted 1:2 in 0.8 M sucrose. Spheroplasts frozen for at least 1-2 weeks appeared to provide consistent results in these experiments. Diluted spheroplasts were then placed on a poly-L-lysine coated glass slide and incubated with equal volume of FITC-labeled peptide (peptide stock concentration of $1.1\text{-}6.2x10^{-4}$M), giving an effective peptide concentration above the MIC for BF2, P11A BF2 and magainin 2 (HipC has effectively no antibacterial activity against *E. coli*). Peptides were typically incubated with spheroplasts for 1 minute, although some samples with HipC were allowed to incubate for 10-20 minutes. All peptides were synthesized at >95% purity by NeoScientific (Cambridge, MA) with a FITC group conjugated at the N-terminus. 1 μL of di-8-ANEPPS (Biotium, Hayward, CA) membrane dye was also added to membrane labeled samples. Spheroplasts were visualized with a Leica TCS SP5 laser scanning confocal microscope with excitation at 488 nm by an argon laser at 20% laser power output and 20% transmission and emission ranges of 499-532 nm (FITC) and 670-745 nm (di-8-ANEPPS). 8-bit, 512x512 images were collected at 63X magnification (Leica Plan-Apochromat oil objective; numerical aperture 1.40). Composite images were produced by Leica LAS AF software (Buffalo Grove, IL). Z-stacks composed of slices with 0.04-0.08 μm thickness were evaluated for localization of peptide

fluorescence within the spheroplast to prevent bias in the reading of the data. Data for each peptide was collected from a minimum of at least two independently prepared batches of spheroplasts characterized over a total of at least five separate imaging sessions for each peptide (Supplemental Tables 1-4). Data was generally consistent between different batches, although a few outliers, particularly one batch incubated with buforin II, emphasizes the need for sufficient replication to robustly characterize peptide mechanisms.

Supplemental Tables

Table 1: Percentages of imaged spheroplasts showing translocation and membrane localization of buforin II (BF2) for different spheroplast batches

	Batch 1	Batch 2	Batch 3	Batch 4
% translocating	83	11	78	85
% membrane localized	17	89	22	15
n of spheroplasts imaged	6	19	9	33

Table 2: Percentages of imaged spheroplasts showing translocation and membrane localization of P11A buforin II (BF2) for different spheroplast batches

	Batch 1	Batch 2	Batch 3	Batch 4	Batch 5
% translocating	60	22	42	21	15
% membrane localized	40	78	58	79	85
n of spheroplasts imaged	5	27	19	24	26

Table 3: Percentages of imaged spheroplasts showing translocation and membrane localization of magainin 2 for different spheroplast batches

	Batch 1	Batch 2
% translocating	17	21
% membrane localized	83	78
n of spheroplasts imaged	46	14

Table 4: Percentages of imaged spheroplasts showing translocation and membrane localization of HipC for different spheroplast batches

	Batch 1	Batch 2	Batch 3	Batch 4
% translocating	71	100	100	100
% membrane localized	28	0	0	0
n of spheroplasts imaged	7	2	22	36

Supplemental Figures

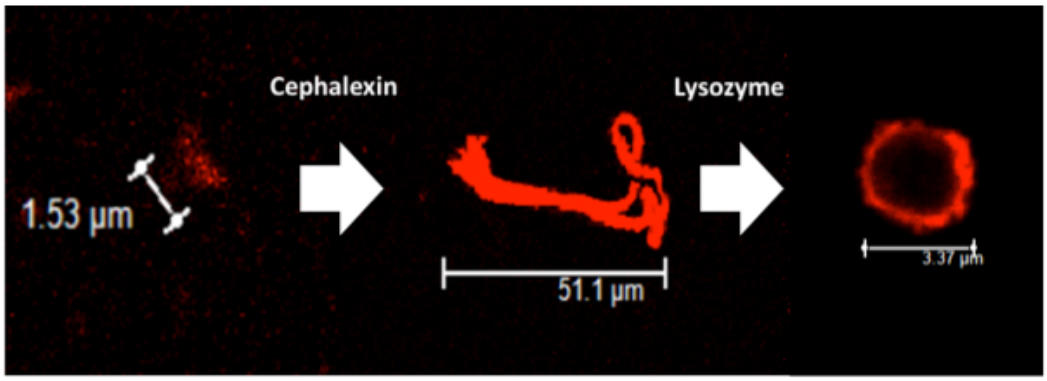

Supplemental Figure 1: Representative confocal microscopy images of *E. coli* at different stages during the formation of spheroplasts. Fluorescence shown is from the membrane dye di-8-ANEPPS.

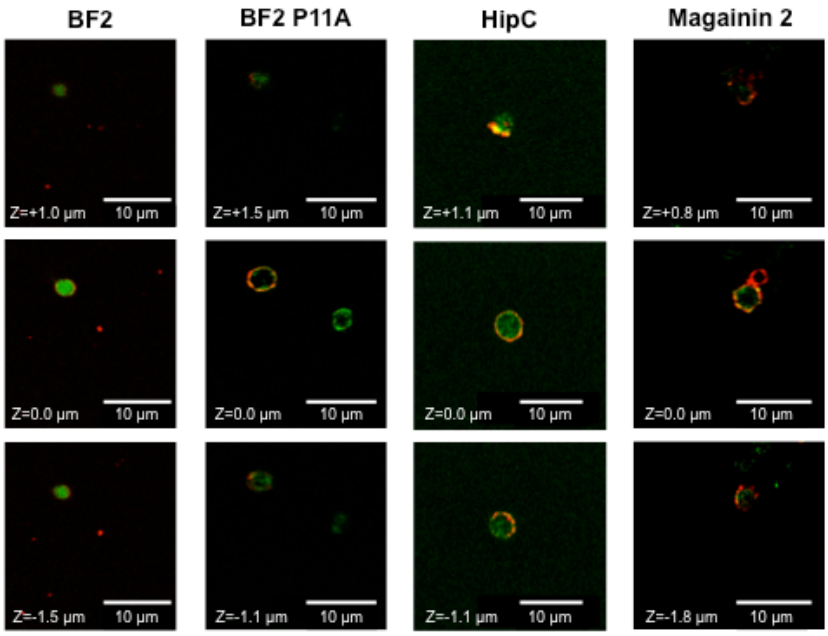

Supplemental Figure 2: Confocal images of representative *E. coli* spheroplasts incubated with FITC labeled peptides (BF2, P11A BF2, HipC or magainin 2) and di-8-ANEPPS. The merged fluorescence of FITC (green) and di-8-ANEPPS (red) is shown. Images from three different positions in a single z-stack are shown for each peptide; z-positions are given relative to the middle image of each stack.

Supplemental Information References

1. **Martinac, B., M. Buechner, A.H. Delcour, J. Adler, and C. Kung**, 1987 Pressure-sensitive ion channel in Escherichia coli. Proc Natl Acad Sci U S A **84**:2297-301.